International Journal of Mass Spectrometry 281 (2009) 134–139

Contents lists available at ScienceDirect

International Journal of Mass Spectrometry

journal homepage: www.elsevier.com/locate/ijms

Twin mass peak ion source for comparative mass spectrometry: Application to circular dichroism laser MS

Christoph Logé, Alexander Bornschlegl, Ulrich Boesl*

Technische Universität München, Chemie Department, Physikalische Chemie, Lichtenbergstrasse 4, 85748 Garching, Germany

ARTICLE INFO

Article history:
Received 8 December 2008
Received in revised form 19 January 2009
Accepted 20 January 2009
Available online 29 January 2009

Keywords:
Time-of-flight mass spectrometry
Resonant laser ionization
Pulsed ion source
Circular dichroism
Dynamic chemical trace analysis

ABSTRACT

A pulsed ion source has been developed supplying two slightly shifted mass spectra for every single ionization pulse, e.g., by laser induced resonance enhanced multiphoton ionization (REMPI). This allows comparison of ion signals with a difference of relative intensity in the percent and sub-percent range. Such small differences may be due to small changes of gas composition or of ionization conditions and usually are hidden by pulse to pulse fluctuations of laser pulse energy, gas density, electric fields, ion detection, etc. With the presented twin-peak ion source, both ion signals are subject to the same fluctuations which will influence the ratio of the ion signals only marginally. This method has been applied to circular dichroism laser mass spectrometry, where relative ion signal ratios $2(I_r - I_l)/(I_r + I_l)$ due to ionization with right and left circularly polarized light have to be recorded in the 10^{-3} range and below.

1. Introduction

A mass spectrometric method to measure two mass spectra in one scan display will be presented. This allows for improved comparison of mass selected ion signals or even whole mass spectra in the case of pulsed ion sources and pulsed mass analyzers. The goal is to enhance the sensitivity for small differences in ion signal and thus study small variations of experimental conditions or distinguish different molecular species such as isomers or enantiomers. There are many practical applications for sensitive comparative mass spectrometry with the ability of time resolution. Some of such applications are synchronized dynamic gas sampling at two different positions with chemical reactions (e.g., catalytic converters) in between or real time analysis and comparison of isomer sensitive chemical or photochemical reactions. This work is focused on application of comparative multiphoton ionization mass spectrometry for enantio-sensitive analysis.

Recently, enantio-sensitive photoionization mass spectrometry has been performed [1,2] by employing pulsed wavelength-tunable nanosecond lasers and time-of-flight mass analyzers. Even the first femtosecond-laser experiments have been reported (K-M. Weitzel, Marburg, private communication, 2007). Enantio-sensitive resonance enhanced multiphoton ionization is achieved by using circularly polarized laser light. This involves circular dichroism in the resonant intermediate absorption step. Circular dichroism is determined by the difference of absorption of left and right handed circularly polarized light by chiral molecules [3]. Its inclusion in the ionization process results in different ion yields for the two entiomers of a chiral molecule. One major problem is that circular dichroism is a very small relative effect. Correspondingly, relative variations $\Delta I/I$ of the ion signal I of 0.001:1 and less have to be measured. Pulse-to-pulse fluctuations of laser pulse energy and spatial laser intensity distribution, but also fluctuations of gas density (e.g., in a molecular beam), electrode potentials in the ion source and electronic noise may exceed these ion signal variations by many times. The idea to overcome this problem is to measure two comparative ion signals or mass spectra, respectively, for every single laser shot. As a consequence, fluctuations on a timescale larger than 10–100 μs (the typical ion flight time in a time-of-flight mass analyzer) will influence both ion signals or mass spectra in a similar way and thus will have a minor effect on the relative variation $\Delta I/I$ of the ion signals.

One possibility to achieve such twin mass spectra is to split one primary pulsed laser beam into two laser beams and to focus them into the ion source of a time-of-flight mass spectrometer. Delaying one of these laser pulses in time by an optical delay line (e.g., 10 m corresponding to $dt = 30$ ns) will give rise to a second mass spectrum delayed by this time dt. Long optical delay lines, however, will change the characteristics of the laser beam strongly and along with it the ionization conditions in the laser focus, in addition to other disadvantages. Our approach to realize a twin mass spectrum technique is based on characteristics of the so-called space focus of pulsed ion sources and will be presented in the following.

* Corresponding author. Tel.: +49 89 289 13397; fax: +49 89 289 14430.
E-mail address: ulrich.boesl@mytum.de (U. Boesl).

1387-3806/$ – see front matter © 2009 Elsevier B.V. All rights reserved.
doi:10.1016/j.ijms.2009.01.008

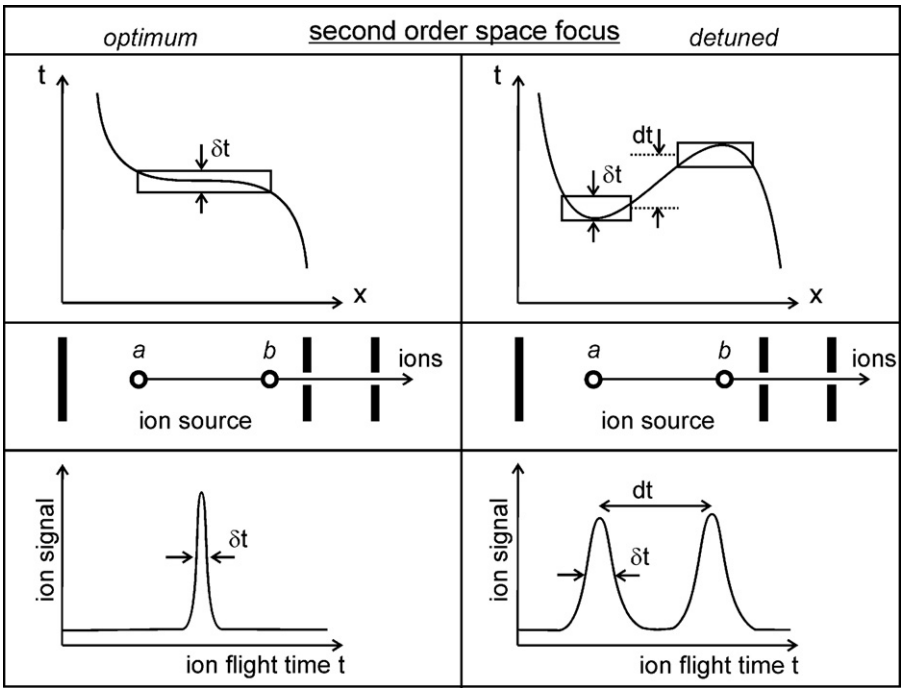

Fig. 1. Space focus of a pulsed ion source with t/x behavior (top), scheme of ion source (middle) and hypothetical ion signal in a time-of-flight mass spectrum (bottom). *Left side*: optimized electrode potentials for a second-order space focus. *Right side:* detuned electrode potentials giving rise to two first order space foci. x: position of ion formation; t: ion flight time as a function of ionization position x; δt: peak width (FWHM) of ion signal; dt: time delay of twin mass peaks. ***a*** and ***b***: two positions of ion formation by laser ionization.

2. Principle of the mass spectrometric twin technique (twin-peak ion source)

The space focus of a pulsed ion source is a position in the field-free drift region behind the ion source where fast ions formed at a position ***a*** in the ion source overtake slow ions formed at a position ***b***. The ion kinetic energy difference caused by different positions of ionization is given by $E\Delta x$ with the electric field E in the region of the ion source where the ions are formed by pulsed laser ionization and are accelerated instantly (constant field) or after a delay time (pulsed field) and a spatial distribution Δx along the ion flight path. The situation of fast ions with one defined mass overtaking slow ions of the same mass is equivalent of the compression of a mass selected ion cloud with all ions of this mass passing the space focus in a narrow time interval δt. This corresponds to a compensation of flight time differences which are due to kinetic energy differences caused by different starting positions and is part of the so-called Wiley McLaren approach [4]. It can be represented graphically in a t/x diagram with t being the ion flight time and x the position of ion formation.

With a two-stage ion source (consisting of three electrodes and two electric fields) a so-called second-order time-to-space compensation (or second-order space focus) can be achieved [5–10]. In this case, ions formed within a wide range of Δx pass the space focus in a particularly narrow time window δt (see Fig. 1 left side). The t/x diagram now represents a third-order polynomial with one flat inflection point (1st and 2nd derivative dt/dx and d^2t/dx^2 are vanishing). The corresponding time-of-flight spectrum (detector at the space focus) is a particularly narrow ion peak even if ions are formed at positions as far apart as positions ***a*** and ***b***.

A second-order space focus is achieved by a well-defined set of electrode potentials and a well defined geometry of the ion source. By detuning these potentials, the t/x diagram represents a third-order polynomial with one pronounced maximum and one pronounced minimum [9]. Compensation of flight time differences is possible in both extrema, although not in second but only in first-order (only 1st order derivative is vanishing). However if the spot of ion formation is small enough reasonable peak widths δt in the time-of-flight mass spectrum are still possible. Small spots of ion formation in the sub-millimeter range are easily achievable by focused laser beams. One has to take care, however, that not space charge effects due to high ion densities are caused by too tight focusing.

As seen from Fig. 1 (right hand side), the flight times of ions formed at position ***a*** and at position ***b*** differ by a time dt. If the peak width δt of ions from spot ***a*** or from spot ***b***, respectively, is considerably smaller than dt mass spectra from both positions are

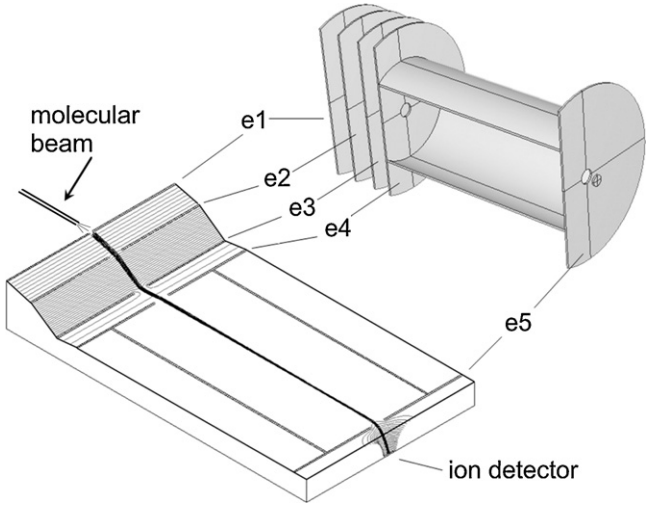

Fig. 2. Scheme of the short time-of-flight mass analyzer and the corresponding SIMION plot of electric field distribution and ion trajectories. e1 to e5: electrodes to which potentials U1 to U4 are applied. Electrodes e4, e5 and the shielding tube are on the same potential U4. The geometric distances are: x(e1–e2) = 13 mm, x(e2–e3) = 13 mm, x(e3–e4) = 10 mm, x(e4–e5) = 124 mm.

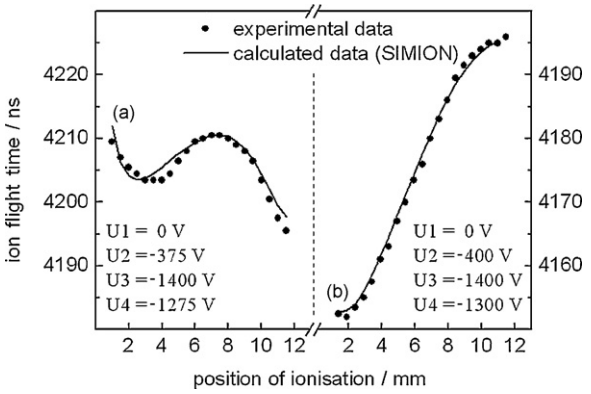

Fig. 3. t/x behavior of a pulsed ion source at two different settings of potentials; (a) nearly second-order focus with dt = 6 ns for ion formation at 3.5 and 7.5 mm. (b) Extrema of $t = f(x)$ are shifted to 2 and 11 mm with dt = 45 ns.

separated and give rise to twin peaks in the time-of-flight mass spectrum. Or in other words: two mass spectra which are slightly shifted in time by dt will be recorded for every single ionization pulse (either laser pulse or electric field extraction pulse). It is this effect which is exploited for the comparative mass spectroscopic twin technique reported here.

3. Experimental setup and test of the principle

Initial experiments have been performed in a small linear time-of-flight mass analyzer with an effusive molecular beam inlet as shown in Fig. 2a. The axis of the effusive beam is collinear with the axis of the analyzer and the ion trajectories, respectively. The ion source consists of three stages (four electrodes e1, e2, e3, e4). This is one stage more than necessary and allows for more flexibility of varying ion source parameters, i.e., potentials U1 to U4 at electrodes e1 to e4. The field-free drift region is a 124 mm long tubing. Its endplate for shielding this region (electrode e5) has a central 8 mm diameter hole so that ions can reach the detector after a final acceleration up to 2300 V between electrode 5 and ion detector. A SIMION [11] simulation of the electric fields and ion trajectories is shown in Fig. 2b.

A laser beam is focused into the effusive molecular beam within the first stage of the ion source. The focusing lens (focal length of 250 mm) is mounted on a micrometer stage which allows its precise movement in a direction vertical to the light beam and parallel to the ion source axis. Thus the laser focus and therefore the spot of ion formation can be moved along the ion source axis in a well defined way. This feature has been used to measure a t/x-diagram. An ArF laser (193 nm) with 5 mJ pulse energy has been focused into a molecular beam of 3-methylcyclopentanone (3-MCP) which absorbs a 193-nm-photon via a $n\sigma^*$-transition and is ionized by absorption of a second 193-nm photon. The chiral molecule 3-MCP exhibits a reasonably large circular dichroism and is therefore a model molecule for our mass spectrometric twin technique.

A t/x-diagram measured with this experimental setup is presented in Fig. 3a together with a SIMION calculation. For the set of electrode potentials {U1 = 0 V, U2 = −375 V, U3 = −1400 V, U4 = −1275 V} a t/x curve has been obtained which is not far from a second-order flight time compensation. The flight time difference of ions from both extrema (at 4 and 8 mm) is only 6 ns. This is smaller than other flight time broadening effects, e.g., the laser pulse length of 10 ns. The measured t/x-diagram is very well reproduced by the SIMION calculations with small deviations of 1–2 ns. No parameters have been adjusted for optimal fit. Detuning the field of the first stage by changing the voltage U2 from −375 to −400 V results in a very strong effect on the t/x-diagram (see Fig. 3b). The flight times of ions from position ***a*** (at 3 mm) and position ***b*** (at 11.5 mm) differ now by 45 ns. Once again, the measured flight times are well represented by the independent SIMION simulation. The field of the third stage of the ion source acts here as a decelerating field and has been slightly optimized for the experiment displayed in Fig. 3b.

In a next experiment, two laser beams have been focused into the first stage of the ion source [12]. These have been formed out of one primary beam via a beam splitter (about 50%/50%). The focus of laser beam 1 has been positioned in front of the ion repelling electrode near the orifice of the molecular beam, the focus of laser beam 2 some 8 mm further downstream. A twin peak with mass 98 due to the molecular ion of 3-MCP is observed, although with strongly differing peak intensities (see Fig. 4a). The flight time difference of both peaks is 50 ns which is by 5 ns more than expected from Fig. 2b. This additional effect is due to the longer pathway of laser beam 2 by 120 cm. This gives rise to a time delay of 4 ns and therefore an ion production time and consequently an ion arrival time shifted by this amount.

The different peak intensities are caused by a considerably lower gas density at position ***b*** due to a spreading out of the effusive gas beam from focus position ***a*** to position ***b***. This is reproduced in the inset of Fig. 4. Here ion numbers are shown which are recorded when the laser focus is shifted from 1 to 12 mm downstream and therefore away from the gas beam orifice. One way to compensate that is by using pulse energies for laser beam 1 which are smaller than that of laser beam 2. By a reduction of the laser pulse energy of beam 1 by more than a factor of 2 the time-of-flight spectrum in Fig. 4b is obtained.

So far, the principle of our mass spectrometric twin-peak method has been proven. However, the situation of strongly differing gas densities at positions ***a*** and ***b*** is unsatisfying. One way to circumvent this problem is to use a perpendicular instead of an inline molecular beam. Positioning the axis of the effusive molecular beam half way between positions ***a*** and ***b*** (see Fig. 1) and the tip of the molecular beam nozzle apart (e.g., by 5 mm) from the ion path will yield equal gas densities at both positions of ionization. This arrangement has been used for the enantio-sensitive series of measurements reported in Section 4. The disadvantage of this set-up is that ionization does not take place at maximum gas density. In the meanwhile, a new double beam inlet system has been developed and constructed in our group, as described in the following.

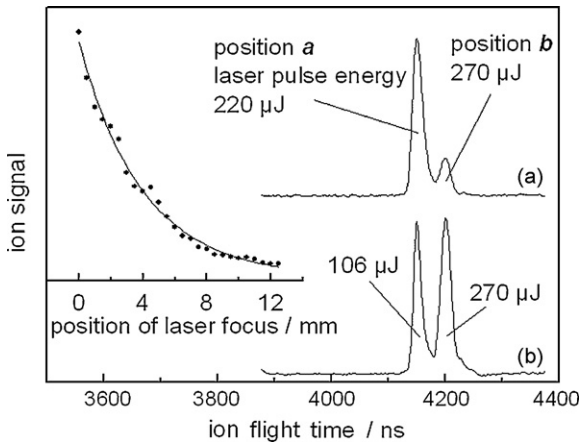

Fig. 4. Twin ion peak mass spectra due to laser ionization at position ***a*** = 2 mm and position ***b*** = 11 mm corresponding to Fig. 3b. (a) Mass spectrum obtained with similar pulse energies of laser beams A and B. The large difference of ion signal intensity is due to the strongly different gas density of an inline molecular beam at both positions (see inset on the left side). (b) Mass spectrum obtained with pulse energies of laser beams A and B matched for equal signal intensities.

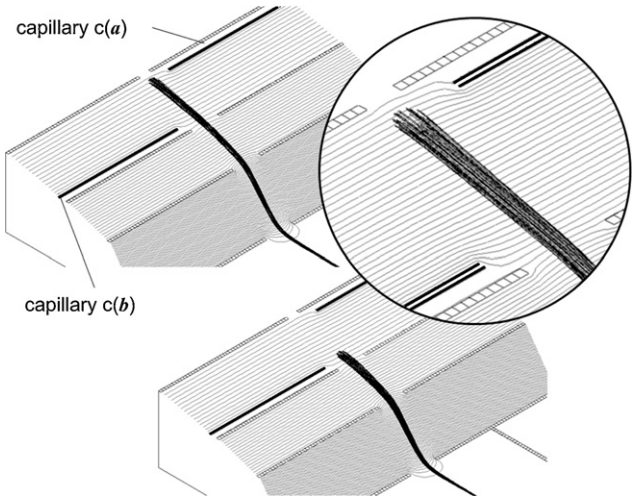

Fig. 5. SIMION simulation with electric field distribution and ion trajectories for an ion source with two effusive gas inlets at ion formation position ***a*** = 2 mm and ***b*** = 11 mm from the repelling electrode e1. The capillaries c(***a***) and c(***b***) are oriented perpendicularly to the ion source axis and thus the direction of ion extraction.

In this double beam inlet system two effusive gas beams are now originating from the tips of two capillaries c(***a***) and c(***b***) with an inner diameter of 0.2 mm reaching into the first ion source region between electrodes e1 and e2. The capillaries are now oriented perpendicularly to the ion source axis and thus the ion trajectories and parallel to the electrodes of the ion source. The tips of the capillaries c(***a***) and c(***b***) have a distance of 3 mm to the ion source axis and therefore to positions ***a*** and ***b*** of ionization. A SIMION simulation of electric fields and ion trajectories starting at positions ***a*** and ***b*** are presented in Fig. 5. These simulations show that ions starting from both positions are well collimated and reach the ion detector with same efficiency despite different inhomogeneities of the electric field near the two capillary tips and despite different ion kinetic energies.

In Fig. 6a, a first mass spectrum obtained with the short time-of-flight mass analyzer with a double effusive gas inlet system is displayed. It consists of two slightly shifted mass spectra of the same molecular species. One problem which shows up immediately when studying Fig. 6 is the limited separation of mass peaks of the first mass spectrum from those of the second mass spectrum as well as mass interferences e.g., of ^{13}C-isotopomers. This may be solved by a longer field-free drift region which results in a larger time-of-flight difference of the twin peaks in addition to a better time-of-flight separation of adjacent mass peaks. In Fig. 6b, the field-free drift region has been extended to a length of 220 mm. The potentials of the electrodes e1, e2 and e3 had to be changed to achieve a corresponding shift of the space focus. It is obvious that for the molecular ion of 3-methylcyclopentanone at mass m/z 98 as well as its fragment at mass m/z 69 a residual overlap of the twin peaks as well as an interference between ^{13}C-isotopomer and twin peak is no problem, anymore. However, due to a "softer" extraction field space charge effects may increase.

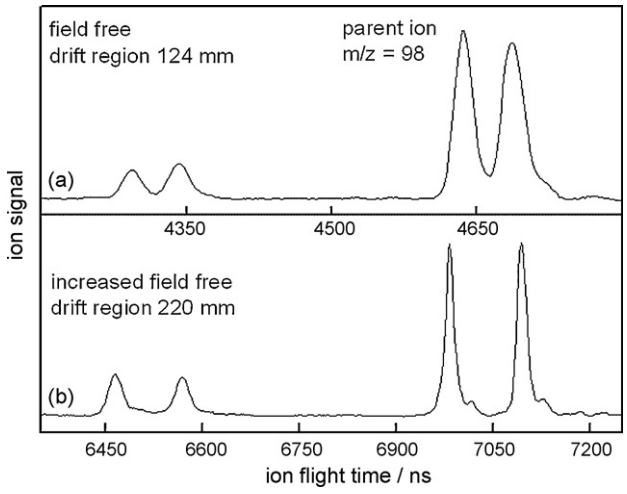

Fig. 6. Twin-peak mass spectra of 3-methylcyclopentanone taken with a double effusive gas inlet and equal pulse energies of laser beams A and B. The ionizing laser wavelength was 193 nm (ArF excimer laser). The mass spectra show the molecular ion (m/z 98) and a major fragment (m/z 69). (a) Mass spectrum taken with the short time-of-flight mass analyzer (see Fig. 1); (b) mass spectrum taken with a time-of-flight mass analyzer with longer field-free drift region and correspondingly adjusted electrode potentials. This results in a better mass resolution, but also a larger shift dt of the twin peaks.

A much more elegant way is the combination of a pulsed "twin-peak ion source" with reflectron time-of-flight mass spectrometry [5–10]. In the optimal compensation mode and for each single ion mass, the ion reflector images the situation in the ion source space focus (as presented in Figs. 3 and 6) to the final ion detector situated in the space focus of the ion reflector [9]. Due to a considerably longer effective flight time, flight time differences of bunches of ions with adjacent mass will now be enlarged by a factor of 10 or even 100. With other words, the double-peak characteristics of the "twin-peak ion source" will be conserved, the mass resolution however will increase significantly. A short distance between ion source and space focus can be chosen which allows higher electric fields at the point of ion formation and thus reduces effects of space charge due to high ion density. Test and further development of this instrumental approach will be the task of future experimental work in our group.

4. Application to mass selective circular dichroism spectroscopy

As mentioned in the introduction, circular dichroism in ion signal instead of absorption or emission has been performed allowing the combination of CD-spectroscopy and mass spectrometry. Since circular dichroism is due to the very small relative difference of absorption, emission or in this case ionization for left and right handed circularly polarized light, even small signal fluctuations may make its observation impossible. This is particularly true when pulsed light sources and pulsed signal detection are involved as in the case of multiphoton ionization with pulsed lasers. Therefore the question arises where the limit of measuring circular dichroism by this new method of CD laser mass spectrometry is and by which means this limit can be reduced.

In this section, investigations of the statistical behavior of the circular dichroism in ion signal $\Delta I/I = 2(I_A - I_B)/(I_A + I_B)$ of 3-methylcyclopentanone are presented using a "twin-peak ion source" with only slightly different potentials as given in Fig. 3b, a single perpendicular effusive gas inlet system (see Section 3) and a pulsed wavelength-tunable laser (Nd:YAG-laser pumped OPO) at 300 nm. Circularly polarized light has been formed by a linear polarizer and a quarter-wave-plate ($\lambda/4$). The circularly polarized light was changed from left handed to right handed by turning the $\lambda/4$-plate by 90°. One single experiment was performed by applying 300 laser pulses split into one beam (A) with left handed circularly polarized light (L-CPL) and one beam (B) with right handed circularly polarized light (R-CPL); in the subsequent experiment 300 laser pulses with changed polarization (beam A: R-CPL and beam B: L-CPL) were applied. This gives rise to two sets of CD-data $\Delta I/I = 2(I_A - I_B)/(I_A + I_B)$ with the ion signals I_A and I_B caused by laser beam A and laser beam B. The two series of measurements

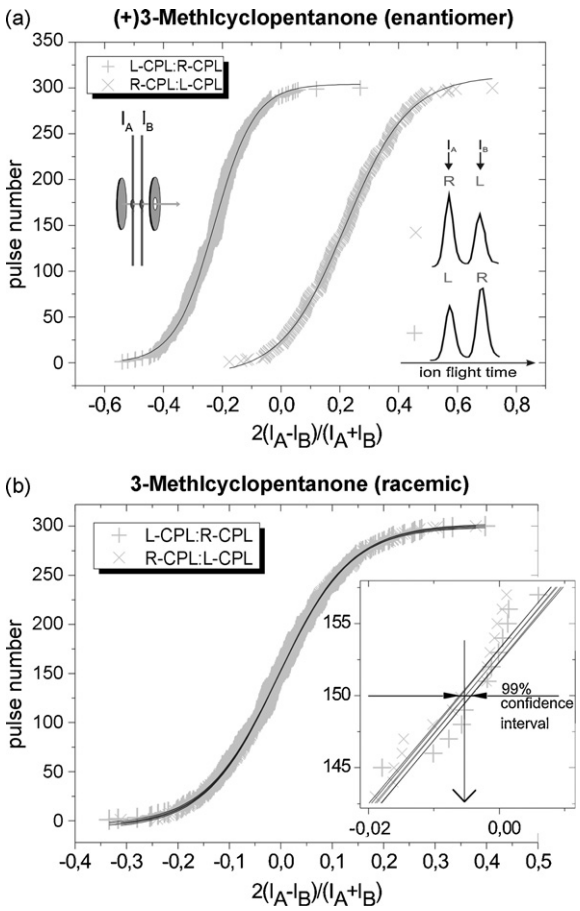

Fig. 7. Circular dichroism in ion signal of 3-methylcyclopentanone (3MCP) measured in a short time-of-flight mass analyzer with twin-peak ion source. Representation is cumulative supplying the integral of the Gaussian distribution. (a) CD in ion signal of the (+)-3MCP enantiomer; left curve: laser beam A is left handed, laser beam B is right handed circularly polarized; right curve: polarizations are vice versa. (b) CD in ion signal of racemic 3MCP. Both curves with interchanged polarizations coincide. *Inset*: The center of (b) on an enlarged scale with the fitted cumulative Gaussian curve and its 99% confidence interval. The CD value in ion signal at pulse number 150 corresponds to the centroid of the Gaussian distribution.

are characterized as L-CPL:R-CPL and R-CPL:L-CPL corresponding to the polarization of beam A and of beam B. A thorough procedure including adjustment of the laser pulse energies has been applied to assure that the ion signals I_A and I_B have equal intensity for linearly polarized light. Consequences of the residual mismatch will be addressed in a subsequent paragraph.

The involved molecular transition of 3-MCP is the $n\pi^*$ transition which is characteristic and similar in wavelength for all ketones (e.g., for formaldehyde as the smallest one [13,14]). This transition may therefore serve for identification of chirality within this important class of molecules. The $n\pi^*$ transition of 3-MCP is known for its large circular dichroism of some 20% [15–17] in conventional CD-spectroscopy and of 27% [18] in multiphoton ionization at 324 nm. The enantiomer (+)-3-methylcyclopentanone has been used which is commercially available and shows enhanced $n\pi^*$-absorption for R-CPL.

For the display of data in Fig. 7 a cumulative presentation has been chosen instead of a histogram for the sake of independence from representation parameters such as the width of histogram channels. For this representation, the values of $\Delta I/I$ of all single 300 measurements have been ordered by their magnitude and numbered from 1 to 300. Displaying the $\Delta I/I$ values on the abscissa and the measurement numbers on the ordinate gives the sigmoidal curves shown in Fig. 7. Applying polarizations "L-CPL:R-CPL" and "R-CPL:L-CPL" to the enantiomer (+)-3-MCP gives rise to the two curves in Fig. 7a; both are well fitted by a Gaussian distribution. The 99% confidence interval is too narrow to be resolved. The centroid of the Gaussian distribution (most probable value of $\Delta I/I$) may be assumed to be at pulse number 150 with sufficient accuracy. Both curves show a centroid with nearly the same absolute value of about 0.19 (the small deviation will be discussed later) but with opposite sign. This is a proof for circular dichroism showing up in multiphoton ionization. As a crosscheck, the same two experiments have been performed with a racemic mixture of 3-methylcyclopentanone. The results are shown in Fig. 7b. The curves of both experiments each consisting of 300 single measurements again are well fitted by a Gaussian distribution. At the scaling of abscissa and ordinate used in Fig. 7b, both curves are not distinguishable and both centroids lie at $\Delta I/I = 0$.

For determining an error margin the curves in Fig. 7 have been analyzed on a larger scale. This did not only supply an error margin but also revealed systematic errors which are not overcome by the twin-peak technique. In the inset of Fig. 7b the central part of Fig. 7b is shown on this enlarged scale. The Gaussian fit curve (central line) and the 99% confidence interval are indicated and appear as linear curves in this small cutout of the curves in Fig. 7b. At pulse number 150 (centroid) the 99% error of $\Delta I/I$ is ±0.8‰. This would mean that circular dichroism laser mass spectrometry has reached a state of development where application to many substances with CD-values in the low and sub-percentage range such as many ketones [3] seems reasonable.

Unfortunately, the centroid in Fig. 7 lies at −5‰, which is beyond the 99% interval around 0‰. In Fig. 7a, the centroids of both curves lie at −0.19 and +0.18, the difference of their absolute values therefore is 10‰ corresponding to a shift of both curves by −5‰ in accordance with Fig. 7b. The major reason for this asymmetry is the residual mismatch of ion signals I_A and I_B in the chiral insensitive situation (e.g., achieved at excitation with linear polarized light). With other words, this residual mismatch is independent of the molecular chirality and therefore an achiral effect. It can be determined with an achiral molecular sample and accounted for when evaluating the enantio-sensitive measurements. When repeating the series of 300 single measurements, erratic shifts of the $\Delta I/I$ value are observed which are even worse and considerably beyond what one would expect from the statistics of single series as in Fig. 7. Obviously, there exist systematic errors which are responsible for an asymmetric variation of ion signals I_A and I_B. We found that the major reasons for these systematic errors are small asymmetric fluctuations of sensitivity and baseline of our dual-channel data acquisition system. Even very small fluctuations are of large importance since small differences of large signals are observed. Of course, these asymmetric variations are independent of molecular chirality. After solving this problem and realizing reflectron ToF-MS with twin mass peak ion source and double gas beam inlet, new series of enantio-sensitive measurements will be performed in our group.

5. Conclusion

We presented a twin-peak ion source by exploiting the t/x (ion flight time to position of ionization) characteristics of a two-stage ion source. We could show, that two mass spectra of the same species could be produced with a flight time difference of 50–100 ns. The corresponding separation of mass peaks is sufficient to confidentially compare the intensities of ion peaks of same mass but due to slightly different ionization or other experimental conditions. Since both ion signals are subject to the same fluctuations of laser pulse energy and geometry, gas flow, electrode potentials, etc. these fluctuations do not influence the relative signal intensity

difference $\Delta I/I$ as strongly as the ion signal I itself. Error margins of $\Delta I/I = \pm 0.8‰$ have been found for ionization experiments involving circular dichroism. These experiments, however, also showed that our method of CD laser mass spectrometry is still subject to systematic errors. These are probably due to small asymmetric fluctuations of the two data acquisition channels. Such problems have to be solved to measure CD values in ion signal of $\Delta I/I < 1‰$ as necessary for most chiral molecules. A further improvement will be achieved by the realization of a twin mass peak ion source reflectron time-of-flight mass spectrometer.

The presented twin mass peak ion source with a double effusive gas inlet system will not only be useful for enantio-sensitive detection but also applicable to dynamic chemical analysis. This will allow to study fast chemical processes by monitoring synchronously chemical species before and after a reaction line. In particular, exhaust cleaning devices of combustion engines such as catalytic converters may be subject of such studies. Resonant laser mass spectrometry has been shown to be well adapted to exhaust emission analysis [19,20]. It allows detection of traces in the ppb range within highly complex gas mixtures and with a time resolution in the 10 ms range.

Acknowledgement

This work has been supported by the Deutsche Forschungsgemeinschaft DFG.

References

[1] R. Li, R. Sullivan, W. Al-Basheer, R.M. Pagni, R.N. Compton, J. Chem. Phys. 125 (2006) 144304.
[2] U. Boesl, A. Bornschlegl, Chem. Phys. Chem. 7 (2006) 2085.
[3] N. Berova, K. Nakanishi, R.W. Woody (Eds.), Circular Dichroism, Principles and Applications, 2nd ed., Wiley-VCH, New York, 2000.
[4] W.C. Wiley, I.H. McLaren, Rev. Sci. Instrum. 26 (1955) 1150.
[5] B.A. Mamyrin, Russian Patent No. 198034 (1966).
[6] B.A. Mamyrin, V.I. Karataev, D.V. Shmikk, V.A. Zagulin, Sov. Phys. JETP 37 (1973) 45.
[7] G.S. Janes, United States Patent No. 3,727,047 (1971).
[8] W. Gohl, R. Kutscher, H.J. Lane, H. Wollnik, Int. J. Mass Spectrom. Ion Phys. 48 (1983) 411.
[9] U. Boesl, R. Weinkauf, E.W. Schlag, Int. J. Mass Spectrom. Ion Proc. 112 (1992) 121.
[10] B.A. Mamyrin, Int. J. Mass Spectrom. Ion Proc. 131 (1994) 1.
[11] SIMION™ Version 8.0, D.J. Manura, D.A. Dahl, Scientific Instrument Services, Inc., Idaho National Laboratory, 2006.
[12] For diverse double excitation schemes with two laser beams in a pulsed ion source see: U. Boesl, R. Weinkauf, C. Weickhardt, E.W. Schlag, Int. J. Mass Spectrom. Ion Proc 131 (1994) 87.
[13] J.C.D. Brand, J. Chem. Soc. (1956) 858.
[14] G.M. Robinson, Can. J. Phys. 34 (1956) 699.
[15] C. Djerassi, R. Records, C. Quannes, J. Jaques, Bull. Soc. Chim. (1966) 2378.
[16] S. Feinleib, F.A. Bovey, J. Chem. Soc. Chem. Commun. (1968) 978.
[17] H.P.J.M. Dekkers, L.E. Closs, J. Am. Chem. Soc. 98 (1976) 2210.
[18] A. Bornschlegl, C. Logé, U. Boesl, Chem. Phys. Lett. 447 (2007) 187.
[19] U. Boesl, R. Weishäupl, W. Thiel, R. Frey, SAE Technical Paper Series 2005-01-0679.
[20] U. Boesl, J. Mass Spectrom. 35 (2000) 289.